Research Square

Preprints are preliminary reports that have not undergone peer review.
They should not be considered conclusive, used to inform clinical practice,
or referenced by the media as validated information.

Multistate Modeling Across the Disease Course in Advanced Stage Classic Hodgkin Lymphoma (cHL): A Report from the HoLISTIC Consortium

Angie Mae Rodday

arodday@tuftsmedicalcenter.org

Tufts Medical Center https://orcid.org/0000-0002-8671-3401

Susan Parsons

Tufts Medical Center

Zhu Cui

Tufts Medical Center

Nicholas Counsell

Cancer Research UK & UCL Cancer Trials Centre

Sara Rossetti

Copenhagen University Hospital

Jenica Upshaw

Beth Israel Deaconess Medical Center

Amy Kirkwood

University College London

James Cerhan

Mayo Clinic College of Medicine and Science https://orcid.org/0000-0002-7482-178X

Jonathan Friedberg

University of Rochester

Andrea Gallamini

Lacassagne Cancer Center

David Hodgson

University Health Network

Peter Johnson

University of Southampton https://orcid.org/0000-0003-2306-4974

John Radford

Christie's Manchester

Deborah Stephens

University of North Carolina https://orcid.org/0000-0001-9188-5008

Matthew Maurer

Mayo Clinic https://orcid.org/0000-0002-1867-0526

Andrew Evens

Rutgers Cancer Institute of New Jersey

Article

Keywords:

Posted Date: November 24th, 2026

DOI: https://doi.org/10.21203/rs.3.rs-11640039/v1

License: This work is licensed under a Creative Commons Attribution 4.0 International License. Read Full License

Additional Declarations: Yes there is potential conflict of interest. AMR: None. SKP: None. ZJC: None. NC: None. SF: None. JU: None. AAK: MSD, Amgen, Pfizer, Autolus, Millennium Takeda, Janssen, Roche, BMS, AZ, BeOne. JRC: None. JWF: None. AG: BMS, Takeda, AbbVie. DH: None. PJ: None. JR: Smith & Nephew, AZ, J&J, Novo-Nordisk, GlaxoSmithKline, Takeda, Novartis, Seagen, SOBI, ADC Therapeutics. DMS: Novartis, Genentech, BeOne, AstraZeneca, AbbVie, Bristol Myers Squibb, BeiGene, Celgene, Pharmacyclics, J&J, Janssen, Pfizer, Eli Lilly. MJM: Bristol Myers Squibb, Roche/Genentech, MD Education. AME: Pharmacyclics, Novartis, Incyte, CRISPR Therapeutics, Pfizer.

Abstract

Pretreatment factors in classic Hodgkin lymphoma (cHL), such as those incorporated into the Advanced Stage Hodgkin Lymphoma International Prognostication Index (A-HIPI), predict outcomes. However, independent contributions by pretreatment factors and early response across the cHL trajectory is unknown. We pooled 1976 adults treated on three advanced stage cHL post-cycle 2 positron emission tomography (PET2)-adapted trials with similar chemotherapy regimens. Multistate modeling (MSM) with Cox regression estimated transition rates, and associated factors, between six states: treatment start (T0), negative PET2, positive PET2, 1-year remission, 5-year treatment failure (TF), and 5-year death. Covariates were the A-HIPI (all transitions) and PET2 (transitions from remission and TF). 81% had negative PET2 and 87% were in 1-year remission. At 5 years, 77% remained in remission, 15% had experienced TF, and 7% had died. Higher risk A-HIPI (per SD) had higher transition rates from T0 to positive PET2 (HR = 1.23, 95%CI = 1.11, 1.35), negative PET2 (HR = 1.42, 95%CI = 1.22, 1.65) or positive PET2 (HR = 1.28, 95%CI = 1.03, 1.59) to TF, remission to TF (HR = 1.30, 95%CI = 1.13, 1.50), and TF to death (HR = 1.48, 95%CI = 1.21, 1.81). Positive PET2 had a higher transition rate from remission to TF (HR = 1.75, 95%CI = 1.20, 2.55). This MSM revealed that pretreatment factors and early response were significant across the cHL trajectory.

Introduction

Advanced stage classic Hodgkin lymphoma (cHL) generally has excellent long-term survival, but a significant minority of patients experience treatment failure, especially when treated with chemotherapy alone. Pre-treatment factors, such as those incorporated into the 1998 International Prognostic Score (1) or the recently enhanced Advanced Stage Hodgkin Lymphoma International Prognostication Index (A-HIPI), predict 5-year overall survival (OS) and progression-free survival (PFS).(2) In addition, the association between early treatment response, often assessed by positron emission tomography (PET), and disease outcomes has been demonstrated.(3, 4) However, the independent prognostic contributions by pretreatment factors and early treatment response analyzed together is unknown, especially their longitudinal impact through the 5-year post-acute disease trajectory.(5)

When analyzing the disease trajectory, methods beyond the traditional Cox proportional hazards (PH) models are needed. Traditional Cox PH models allow us to estimate the associations between baseline covariates with a single time-to-event outcome while accounting for censoring, with extensions to incorporate time-varying covariates and multiple competing events. If time-varying covariates are not accounted for appropriately, they may result in immortal time bias where survival time is inflated differentially because patients must survive to a certain time point (“immortal time”).(6) Further, in the presence of competing risks (e.g., death prevents treatment failure), the assumption of non-informative censoring is violated because those who are censored due to the competing risk (e.g., death) are not represented by those who continue to be followed.(7) This issue is often addressed through use of composite endpoints (e.g., PFS).(8) However, these traditional survival analyses, even those incorporating time-varying covariates and competing risks, collapse heterogeneous clinical pathways,

obscuring the dynamic sequence of remission, treatment failure, and death. The use of multistate models (MSM) overcome these challenges by explicitly modeling transitions between clinically meaningful disease states while allowing for different covariates for each transition, time-varying covariates, and competing risks. This methodology is useful for answering important and dynamic clinical questions about the disease trajectory in cHL and has been applied to other hematological malignancies or solid tumors.(9–11)

Adriamycin (doxorubicin), bleomycin, vinblastine, and dacarbazine (ABVD) has been a standard treatment regimen for cHL for nearly 30 years across many parts of the world.(12) Over the past 15 years, the use of early/interim PET has guided response-adapted treatment escalation or de-escalation, aimed at reducing chemotherapy toxicity.(13) More recently, targeted therapeutic agents have been integrated into the frontline setting (i.e., antibody drug conjugates and checkpoint inhibitors). However, many parts of the world do not have access to these targeted agents in the frontline setting, and standard therapy remains multiagent chemotherapy, such as ABVD.

Through the *HoLISTIC* (Hodgkin Lymphoma International Study for Individual Care) consortium, detailed individual patient data have been obtained from seminal, phase III, international cHL clinical trials and global cHL registries and have been harmonized, standardized, and normalized using a common data model with detailed data dictionary.(14) Harnessing this rich multi-source data and MSM, we examined outcomes across the post-acute disease trajectory and assessed whether pretreatment factors (as measured by the A-HIPI) and early disease response (as measured by the PET2) provided independent information about the trajectory among patients with advanced stage cHL enrolled in contemporary PET-adapted, ABVD-based clinical trials.

Methods

Data Sources and Study Population

We obtained and harmonized individual patient data through separate formal data sharing agreements with international cHL clinical trial groups. The Tufts Health Sciences Institutional Review Board determined this to be not human subjects research. To better align the patients across multiple trials, this analysis was restricted to patients aged 18–65 years with stage IIB, III, or IV cHL who were treated on advanced stage, post-cycle 2 PET (PET2)-adapted phase III clinical trials (GITIL HD0607,(15) SWOG0816(16), UK RATHL(17)) (**Table S1, Figure S1**). All patients first received 2 cycles of ABVD; those with a negative PET2 (Deauville score (DS) ≤ 3)(18) received ABVD or AVD (ABVD without bleomycin). Therapy for those with a positive PET2 (DS > 3) was escalated to BEACOPP (bleomycin, etoposide, Adriamycin/doxorubicin, cyclophosphamide, Oncovin/vincristine, procarbazine, prednisone).

Multistate modeling (MSM) and disease states

MSM describes how individuals move among a series of disease states over time. This includes the probability of being in a disease state at a given time, the probability of transitioning between disease states, and determining which covariates are associated with transition rates between disease states. (19, 20) Our MSM had six disease states (Fig. 1): treatment start (time 0), negative PET2, positive PET2, remission after initial treatment, treatment failure, and death. All patients enter the model at the treatment start state and can transition forward to other states without returning to prior states; death by 5 years was considered the final absorbing state.

Given that PET2 occurred after two cycles of ABVD, time-to-transition to negative or positive PET2 was set to 60 days; those who were lost to follow-up before their PET2 or experienced an event (n = 57, Fig. 1) were censored at their date of last known follow-up. Only 5 patients transitioned directly from treatment start to treatment failure (n = 2) or death (n = 3) prior to the planned PET2 (Fig. 1). Remission after initial treatment was defined as not experiencing treatment failure or death ≤ 1 year after start of treatment. Given varying lengths of treatment regimens and assessment of end of treatment response, the time-to-reach remission after initial treatment was set to 1 year for all patients reaching that state. Patients with unknown disease status at 1 year were censored at their date of last known follow-up. Treatment failure was defined as progression or relapse. Death was defined as death from any cause. We used the adjudication of outcomes from the original data sources. Entry into the treatment failure or death state incorporated the actual timing of the event. Remaining patients were censored at their date of last known follow-up or at 5 years.

Covariates

To operationalize assessment of the independent associations between pre-treatment factors and early disease response with the disease states, the two covariates of interest were the baseline A-HIPI PFS score and PET2 status. The A-HIPI PFS (comprised of baseline stage and continuous age, lymphocyte count, and albumin) is typically scored so that higher values represent a higher probability of being event-free at 5 years (i.e., higher values are better).(2) For this analysis, the A-HIPI PFS was “reverse” scored so that higher values indicate a higher probability of experiencing a 5-year PFS event (i.e., higher values are worse); this was then modeled for a 1-standard deviation (SD) increase for transitions between all modeled MSM disease states. In addition to being considered as disease states in the MSM, PET2 status (positive vs. negative) was also included as a covariate in transitions from remission at 1 year and from treatment failure.

Statistical analysis

The MSM was estimated using a Cox proportional hazards (PH) model with the Breslow method for ties; (19–21) each transition had its own baseline hazard function.

We first fit a non-parametric model without covariates to estimate transition hazards and probabilities, and their variances based on the Aalen estimator, which were used to calculate the probability of being in

a given state at a given time (i.e., state occupancy).(19, 20) Our approach was based on the clock forward direction where time moves forward from the initial state, representing a Markov model where the future depends on the present state.

Next, we extended this approach to create semi-parametric models to include transition-specific covariates and estimate hazard ratios (HR) describing the association between covariates and a given transition between disease states. Transitions with < 5 events were not included in this part of the analysis due to unstable estimates (as shown in red in Fig. 1). Furthermore, patients entering the "remission at 1 year" state were forced to enter at that time so excluded from this part of the analysis. Instead, information about those not entering remission at 1 year was attained by the actual timing of transitions into treatment failure or death. Univariable models were estimated for A-HIPI PFS (all transitions) and PET2 results (transitions from remission at 1 year and from treatment failure), and then both were combined into a multivariable model.

We created state occupancy plots by tertiles of A-HIPI PFS score (low risk, mid risk, high risk) and PET2 result to demonstrate differences in the probability of being in a given state at a given time by these key factors.

Missingness of A-HIPI PFS variables was minimal (2%), so a complete case analysis was performed. A two-sided alpha of 0.05 was used. Statistical analyses were performed using R (version 5.5.2)/RStudio(2024.09.1) with the following packages: tidyverse, survival, mstate, ggplot2, and gtsummary.

Results

Among 1 967 eligible participants (Figure S1), median age was 32 years (interquartile range, IQR = 25–43), 53% were male, 28% were stage IIB, 37% were stage III and 35% were stage IV. Mean A-HIPI PFS score, which estimated the risk of experiencing a 5-year PFS event, was 22.9% (SD = 6.5%) (Table 1, **Table S2**). Median follow-up was 57 months (IQR = 39–60).

Table 1
Study population, n = 1 967

Clinical trial, n (%) [a]	**Summary statistic**
GITIL HD0607	736 (37.4%)
SWOG0816	322 (16.4%)
UK RATHL	909 (46.2%)
Age (years), mean (SD)	34.8 (12.1)
Age (years), median (IQR)	32.0 (25.0–43.0)
Female sex, n (%)	925 (47.0%)
Stage, n (%)	
IIB	548 (27.9%)
III	722 (36.7%)
IV	697 (35.4%)
B symptoms, n (%)	1 464 (74.4%)
Histology, n (%)	
Lymph Depleted	16 (0.8%)
Lymph Rich	42 (2.1%)
Mixed Cellularity	236 (12.0%)
Nodular Sclerosis	1 405 (71.4%)
NOS or unknown cHL subtype	268 (13.6%)
Bulky disease [b]	492 (25.1%)
WBC count (10^3/uL), mean (SD)	11.2 (5.1)

Abbreviations: ESR, erythrocyte sedimentation rate; IQR=interquartile range; NOS, not otherwise specified; SD, standard deviation; WBC, white blood cell.

[a] Number of patients by trial and registry refer to the subset of patients who met the eligibility criteria for the analytic cohort (**Figure S1**).

[b] Bulk disease defined according to each trial (any mass ≥ 10 cm for GITIL HD0607 and SWOG0816; >1/3 thoracic diameter for mediastinal mass or > 10cm for non-mediastinal mass for UK RATHL)

Missingness: 852 missing ESR, missingness for rest of variables is < 10

Clinical trial, n (%) [a]	Summary statistic
Lymphocyte count (10^3/uL), mean (SD)	1.5 (0.7)
Hemoglobin (g/dL), mean (SD)	12.0 (1.8)
Albumin (g/dL), mean (SD)	3.7 (0.6)
ESR (mm/hr), mean (SD)	57.9 (35.8)
5-year A-HIPI probability of PFS event, mean (SD)	22.9 (6.5)
5-year A-HIPI probability of being PFS event-free, mean (SD)	77.1 (6.5)
Abbreviations: ESR, erythrocyte sedimentation rate; IQR=interquartile range; NOS, not otherwise specified; SD, standard deviation; WBC, white blood cell.	
[a] Number of patients by trial and registry refer to the subset of patients who met the eligibility criteria for the analytic cohort (**Figure S1**).	
[b] Bulk disease defined according to each trial (any mass ≥ 10 cm for GITIL HD0607 and SWOG0816; >1/3 thoracic diameter for mediastinal mass or > 10cm for non-mediastinal mass for UK RATHL)	
Missingness: 852 missing ESR, missingness for rest of variables is < 10	

Figure 1 presents how patients move through the MSM, including the number of people entering each state, remaining in the state (due to censoring, **Table S3**), and transitioning to a future state. At PET2 (60 days), 80.5% (95%CI = 80.3%, 80.6%) of patients had a negative result and 16.9% (95%CI = 16.9%, 17.0%) had a positive result (Fig. 2). At 1 year, 86.5% (95%CI = 85.1%, 87.8%) had achieved remission. At 5 years, 77.2% (95%CI = 75.4, 79.1) were still in remission, 15.4% (95%CI = 13.6, 17.4) had experienced treatment failure, and 7.1% (95%CI = 5.9%, 8.6%) had died.

A-HIPI PFS and PET2 results from MSM

Higher risk A-HIPI PFS scores (per SD) were associated with higher transition rates (as indicated by higher HRs) from treatment start to positive PET2 (HR = 1.23, 95%CI = 1.11–1.35) and from both negative PET2 (HR = 1.42, 95%CI = 1.22, 1.65) and positive PET2 (HR = 1.28, 95%CI = 1.03, 1.59) to treatment failure (Table 2, Figure S2). When adjusting for PET2 result, higher risk A-HIPI PFS scores (per SD) were associated with higher transition rates from remission to treatment failure (HR = 1.30, 95%CI = 1.13, 1.50) and from treatment failure to death (HR = 1.48, 95%CI = 1.21, 1.81). A similar relationship between higher risk A-HIPI PFS score and transitioning from remission to death was found, but, with fewer events observed, this did not reach statistical significance (HR = 1.77, 95%CI = 0.91–3.45).

Table 2
Hazard ratios (HR) of transitioning between disease states for A-HIPI PFS and PET2 from multistate Cox PH model

Transition		Univariable		Multivariable (A-HIPI PFS and PET2)	
	Variable	HR (95% CI)	p-value	HR (95% CI)	p-value
T0 → PET2-	Higher risk A-HIPI PFS [a]	0.94 (0.89, 0.99)	0.02	0.94 (0.89, 0.99)	0.02
T0 → PET2+	Higher risk A-HIPI PFS [a]	1.23 (1.11, 1.35)	< 0.01	1.23 (1.11, 1.35)	< 0.01
PET2- → Treatment Failure	Higher risk A-HIPI PFS [a]	1.42 (1.22, 1.65)	< 0.01	1.42 (1.22, 1.65)	< 0.01
PET2+ → Death	Higher risk A-HIPI PFS [a]	1.38 (0.69, 2.76)	0.36	1.38 (0.69, 2.76)	0.36
PET2+ → Treatment Failure	Higher risk A-HIPI PFS [a]	1.28 (1.03, 1.59)	0.02	1.28 (1.03, 1.59)	0.02
Remission → Treatment Failure	Higher risk A-HIPI PFS [a]	1.32 (1.14, 1.51)	< 0.01	1.30 (1.13, 1.50)	< 0.01
Remission → Death	Higher risk A-HIPI PFS [a]	1.78 (0.92, 3.44)	0.09	1.77 (0.91, 3.45)	0.09
Treatment Failure → Death	Higher risk A-HIPI PFS [a]	1.50 (1.22, 1.83)	< 0.01	1.48 (1.21, 1.81)	< 0.01
Remission → Treatment Failure	PET2 + v PET2-	1.84 (1.27, 2.69)	< 0.01	1.75 (1.20, 2.55)	< 0.01
Remission → Death	PET2 + v PET2-	1.61 (0.18, 14.45)	0.67	1.46 (0.16, 13.07)	0.74
Treatment Failure → Death	PET2 + v PET2-	1.60 (0.98, 2.61)	0.06	1.53 (0.93, 2.49)	0.09

See Fig. 1 for MSM structure. The multivariable results for the first 5 rows are the same as the univariable results because PET2 status was not included for these early transitions that include entering or exiting the PET2 disease states.

[a] A-HIPI PFS HR interpreted for 1 SD increase in score (where higher A-HIPI PFS score indicates higher probability of PFS event).

Those with positive PET2 had a higher transition rate from remission to treatment failure (HR = 1.75, 95%CI = 1.20, 2.55) as compared to those with negative PET2, when adjusting for A-HIPI PFS score. The

relationship between positive PET2 and transitioning from treatment failure to death (HR = 1.53, 95% CI 0.93–2.49) did not reach statistical significance. With only 5 patients transitioning from remission to death, estimates for the adjusted relationship between PET2 status and this transition showed uncertainty, as indicated by the wide confidence interval (HR = 1.46, 95%CI = 0.16, 13.07).

MSM state occupancy by A-HIPI PFS and PET2 result

The probability of being in a given state at a given time by A-HIPI PFS tertile and PET2 result is demonstrated in Fig. 3. Both A-HIPI PFS tertile and PET2 result changed the probabilities of being in remission, treatment failure, and death over time, with A-HIPI PFS tertiles appearing to have a larger impact than PET2 result.

Discussion

In this pooled individual patient-level analysis of advanced-stage cHL patients treated on ABVD PET2-adapted trials, we developed an MSM that refines prognostication across the post-acute disease trajectory by integrating baseline clinical risk (A-HIPI PFS) and early treatment response (PET2). Several important findings emerged from this work. First, the baseline A-HIPI PFS—originally derived to predict 5-year PFS using pretreatment variables for newly-diagnosed patients—was significantly associated with early treatment response and retained significance in first remission and in the relapse setting even after early treatment response was known. Second, PET2 provided independent prognostic information beyond baseline risk provided by the A-HIPI PFS. Together, these findings highlight the usefulness of MSM in demonstrating how both baseline clinical risk and early treatment response are significant prognostic factors throughout the cHL post-acute disease trajectory.

Our findings extend prior work establishing the prognostic value of PET2 in cHL PET-adapted treatment strategies such as HD0607,(15) RATHL(17) and SWOG S0816.(16) Not only has interim metabolic response assessed via PET been widely adopted as a dynamic marker guiding escalation or de-escalation of therapy, but prior analysis using Cox PH modeling found that baseline risk as measured by the International Prognostic Score was no longer significantly associated with PFS once PET2 results were known.(4) However, assessing baseline risk using the A-HIPI PFS, which outperforms the International Prognostic Score ,(2) and utilizing MSM allow for advancement in understanding of factors affecting the post-acute disease trajectory. Notably, the present MSM framework shows that baseline A-HIPI PFS continues to influence downstream disease transitions even after accounting for PET2, supporting a model of multi-modal prognostication in which clinical host and disease factors shape both chemosensitivity and post-remission durability. Clinically, this suggests that reliance on PET2 alone incompletely captures relapse risk, particularly among patients with unfavorable disease who achieve early metabolic response.

The use of MSM methodology represents an important conceptual advance for the modeling of clinical outcomes in the cHL post-acute disease trajectory.(19, 20) Traditional Cox PH models are limited to a

single time-to-event outcome, which can obscure the heterogenous sequence of remission, treatment failure, and death. MSM not only allows us to estimate transitions between these distinct disease states, but also to incorporate different covariates into these transitions. MSMs have recently been utilized in other hematological malignancies to investigate patient heterogeneity that is often oversimplified in traditional Cox PH models.(9–11) For example, Maura et al combined clinical, demographic, genomic, and therapeutic data in an MSM that included states for remission, progression, and death to improve prognostication of outcomes for patients with newly diagnostic multiple myeloma compared to existing prognostic models.(11)

The transition-specific HRs observed herein, particularly the persistent protective effect of lower risk A-HIPI PFS scores across multiple transition states over the disease course, highlight the value of this approach for disentangling how and when prognostic factors exert influence. Moreover, the ability to generate patient-specific estimates of 5-year treatment failure based on a combination of baseline clinical factors and early treatment response illustrates the potential clinical utility and robustness of MSM-based prediction.

These findings have several implications for clinical decision-making and trial design. Risk-adapted strategies in advanced-stage cHL have historically focused on treatment intensity modification according to early treatment response, yet our results suggest that integrating pretreatment risk may further refine personalization.(22) For example, patients with discordant features, such as negative PET2 but high-risk A-HIPI PFS, may warrant closer surveillance or consideration of further consolidation strategies. Conversely, those with negative PET2 and low-risk A-HIPI PFS demonstrate relatively low predicted treatment-failure risk, reinforcing the safety of de-escalation approaches. MSM-derived transition probabilities could also inform future adaptive or response-stratified trial designs, survivorship planning, and individualized care counseling by providing time-dependent, individualized outcome estimates rather than static cohort-level survival rates.

Several limitations warrant consideration. Although these results are based on three large prospective trials with standardized PET2-adapted therapy and high follow-up rates through 5 years, the cohort reflects clinical trial populations aged ≤ 65 years and may not generalize to older or more frail patient populations. Treatment approaches have also continued to evolve, including the incorporation of novel targeted therapeutic agents (e.g., brentuximab vedotin, checkpoint inhibitors) into frontline regimens, which were not represented here, but could be included in future analyses. Of note, the A-HIPI clinical prediction tool was recently shown to perform well in the S1826 trial incorporating novel agents (antibody drug conjugates and checkpoint inhibitors) for adults with advanced-stage cHL(23) and was comparable in performance to the original ABVD-treated cohort.(2) In addition, salvage therapies and post-relapse management among those with treatment failure on the highlighted trials were heterogeneous and not explicitly modeled, which could potentially influence key transitions from treatment failure to death. Even with nearly 2000 patients, analyses of less common transitions were likely underpowered (e.g., PET2 or remission to death) and we were unable to estimate all transitions due to a small number of events. Given the differential length of treatment regimens included in this analysis,

remission was defined at 1 year and transitions from PET2 into that state were not explicitly modeled, but complementary information was attained from transitions from PET2 into treatment failure or death. Remission at 1 year was nevertheless included in the MSM to indicate whether patients reached this state and to model transitions out of remission. While our MSM improves representation of disease dynamics, its predictive performance and calibration in external datasets remain to be established. Finally, newer predictive markers of early treatment response, such as ctDNA and radiomic features,(24) should also be analyzed in the context of MSM.

Altogether, this study demonstrates that integrating baseline clinical risk, such as the A-HIPI, with early treatment response using a MSM framework provides a comprehensive understanding of outcome heterogeneity in advanced-stage cHL. The independent and persistent prognostic contributions of both A-HIPI and PET2 support a multidimensional approach to risk stratification across the disease course. Future work should extend MSM-based prediction to contemporary therapeutic platforms, integrate newer predictive markers such as ctDNA and radiomics features, incorporate salvage and survivorship outcomes, and prospectively evaluate individualized decision support tools derived from these models across the disease course.

Declarations

Competing Interests:

This work was supported by a grant from the National Cancer Institute grant number, R01 CA 262265-05 (Modeling Multi-Source Data in Hodgkin Lymphoma; mPIs SKP and AME).

Author Contributions:

AMR was responsible for conceiving and designing the work that led to this submission, interpreting the results, drafting the manuscript, approving the final version, and is accountable for all aspects of the work. SKP was responsible for conceiving and designing the work that led to this submission, acquiring data, interpreting the results, drafting the manuscript, approving the final version, and is accountable for all aspects of the work. ZJC, NC, SR, JNU, JRC, DH, JR, were MJM were responsible for interpreting the results, revising the manuscript, approving the final version, and are accountable for all aspects of the work. AAK, JWF, AG, PJ, and DMS were responsible for acquiring data, interpreting the results, revising the manuscript, approving the final version, and are accountable for all aspects of the work. AME was responsible interpreting the results, drafting the manuscript, approving the final version, and is accountable for all aspects of the work.

Acknowledgements:

We gratefully acknowledge the HoLISTIC Consortium for providing patient data and for their contributions to the analysis and scientific development of this manuscript. We acknowledge Rachel Murphy-Banks, MA for assistance with project management and manuscript preparations; and Qingyan Xiang, PhD, for his early contributions to statistical analyses.

Data Availability:

The data that support the findings of this study were made available from the leaders of each of the clinical trials (GITIL HD0607: AG; SWOG0816: DS, JF; UK RATHL: PMJ), but restrictions apply to the availability of these data, which were used under data use agreements for the current study, and so are not publicly available.

References

1. Hasenclever D, Diehl V, Armitage JO, Assouline D, Björkholm M, Brusamolino E, et al. A Prognostic Score for Advanced Hodgkin's Disease. N Engl J Med. 1998;339(21):1506–14. doi:10.1056/NEJM199811193392104
2. Rodday AM, Parsons SK, Upshaw JN, Friedberg JW, Gallamini A, Hawkes E, et al. The Advanced-Stage Hodgkin Lymphoma International Prognostic Index: Development and Validation of a Clinical Prediction Model From the HoLISTIC Consortium. J Clin Oncol. 2023;41(11):2076–86. doi:10.1200/JCO.22.02473
3. Hutchings M, Loft A, Hansen M, Pedersen LM, Buhl T, Jurlander J, et al. FDG-PET after two cycles of chemotherapy predicts treatment failure and progression-free survival in Hodgkin lymphoma. Blood. 2006;107(1):52–9. doi:10.1182/blood-2005-06-2252
4. Gallamini A, Hutchings M, Rigacci L, Specht L, Merli F, Hansen M, et al. Early Interim 2-[^{18} F]Fluoro-2-Deoxy-D-Glucose Positron Emission Tomography Is Prognostically Superior to International Prognostic Score in Advanced-Stage Hodgkin's Lymphoma: A Report From a Joint Italian-Danish Study. J Clin Oncol. 2007;25(24):3746–52. doi:10.1200/JCO.2007.11.6525
5. Evens AM, Parsons SK. Continuum of Care for Hodgkin Lymphoma: Impact of Modern Therapy on Postacute Morbidity and Mortality. J Clin Oncol. 2020;38(35):4131–4. doi:10.1200/JCO.20.02668
6. Suissa S. Immortal Time Bias in Pharmacoepidemiology. Am J Epidemiol. 2008;167(4):492–9. doi:10.1093/aje/kwm324
7. Austin PC, Lee DS, Fine JP. Introduction to the Analysis of Survival Data in the Presence of Competing Risks. Circulation. 2016;133(6):601–9. doi:10.1161/CIRCULATIONAHA.115.017719
8. Manja V, AlBashir S, Guyatt G. Criteria for use of composite end points for competing risks—a systematic survey of the literature with recommendations. J Clin Epidemiol. 2017;82:4–11. doi:10.1016/j.jclinepi.2016.12.001

9. Çağlayan Ç, Goldstein JS, Ayer T, Rai A, Flowers CR. A population-based multistate model for diffuse large B-cell lymphoma–specific mortality in older patients. Cancer. 2019;125(11):1837–47. doi:10.1002/cncr.31981
10. Çağlayan Ç, Terawaki H, Ayer T, Goldstein JS, Rai A, Chen Q, et al. Assessing the Effectiveness of Treatment Sequences for Older Patients With High-risk Follicular Lymphoma With a Multistate Model. Clin Lymphoma Myeloma Leuk. 2019;19(5):300–309.e5. doi:10.1016/j.clml.2018.12.019
11. Maura F, Rajanna AR, Ziccheddu B, Poos AM, Derkach A, Maclachlan K, et al. Genomic Classification and Individualized Prognosis in Multiple Myeloma. J Clin Oncol. 2024;42(11):1229–40. doi:10.1200/JCO.23.01277
12. Bonadonna G, Zucali R, Monfardini S, De Lena M, Uslenghi C. Combination chemotherapy of Hodgkin's disease with adriamycin, bleomycin, vinblastine, and imidazole carboxamide versus MOPP. Cancer. 1975;36(1):252–9. doi:10.1002/1097-0142(197507)36:1%3C252::AID-CNCR2820360128%3E3.0.CO;2-7
13. Evens AM. Newly Diagnosed Classical Hodgkin Lymphoma: Optimizing Outcomes in a New Therapeutic Era. Hematol Oncol. 2025;43(S2):e70066. doi:10.1002/hon.70066
14. Parsons SK, Rodday AM, Upshaw JN, Scharman CD, Cui Z, Cao Y, et al. Harnessing multi-source data for individualized care in Hodgkin Lymphoma. Blood Rev. 2024;65:101170. doi:10.1016/j.blre.2024.101170
15. Gallamini A, Tarella C, Viviani S, Rossi A, Patti C, Mulé A, et al. Early Chemotherapy Intensification With Escalated BEACOPP in Patients With Advanced-Stage Hodgkin Lymphoma With a Positive Interim Positron Emission Tomography/Computed Tomography Scan After Two ABVD Cycles: Long-Term Results of the GITIL/FIL HD 0607 Trial. J Clin Oncol. 2018;36(5):454–62. doi:10.1200/JCO.2017.75.2543
16. Press OW, Li H, Schöder H, Straus DJ, Moskowitz CH, LeBlanc M, et al. US Intergroup Trial of Response-Adapted Therapy for Stage III to IV Hodgkin Lymphoma Using Early Interim Fluorodeoxyglucose–Positron Emission Tomography Imaging: Southwest Oncology Group S0816. J Clin Oncol. 2016;34(17):2020–7. doi:10.1200/JCO.2015.63.1119
17. Johnson P, Federico M, Kirkwood A, Fosså A, Berkahn L, Carella A, et al. Adapted Treatment Guided by Interim PET-CT Scan in Advanced Hodgkin's Lymphoma. N Engl J Med. 2016;374(25):2419–29. doi:10.1056/NEJMoa1510093
18. Barrington SF, Mikhaeel NG, Kostakoglu L, Meignan M, Hutchings M, Müeller SP, et al. Role of Imaging in the Staging and Response Assessment of Lymphoma: Consensus of the International Conference on Malignant Lymphomas Imaging Working Group. J Clin Oncol. 2014;32(27):3048–58. doi:10.1200/JCO.2013.53.5229
19. Putter H, Fiocco M, Geskus RB. Tutorial in biostatistics: competing risks and multi-state models. Stat Med. 2007;26(11):2389–430. doi:10.1002/sim.2712
20. De Wreede LC, Fiocco M, Putter H. The mstate package for estimation and prediction in non- and semi-parametric multi-state and competing risks models. Comput Methods Programs Biomed.

2010;99(3):261–74. doi:10.1016/j.cmpb.2010.01.001

21. Breslow N. Covariance Analysis of Censored Survival Data. Biometrics. 1974;30(1):89. doi:10.2307/2529620
22. Maurer MJ, Parsons SK, Upshaw JN, Rodday AM, Mwangi R, Rossetti S, et al. The A-HIPI prediction model in advanced-stage Hodgkin lymphoma: identification of risk groups and creation of an online tool. Blood Adv. 2025;9(6):1366–9. doi:10.1182/bloodadvances.2024014689
23. Casulo C, Li H, Herrera A, Castellino S, Rutherford S, Davison K, et al. Clinical prognostication in the SWOG 1826 randomized clinical trial of nivolumab-AVD versus brentuximab-AVD: Performance of the advanced-stage Hodgkin lymphoma international prognostic index (A-HIPI). Blood. 2025;146(Supplement 1):154–154. doi:10.1182/blood-2025-154
24. Ferdinandus J, Rossi C, Kaul H, Leiders S, Casasnovas O, Ghesquieres H, et al. 12 | IMAGING BIOMARKERS FOR THE DEFINITION OF RESPONSE IN THE GHSG HD18, GHSG HD21 AND LYSA AHL2011 TRIALS FOR ADVANCED-STAGE HODGKIN LYMPHOMA. Hematol Oncol. 2025;43(S3):e12_70093. doi:10.1002/hon.70093_12

Figures

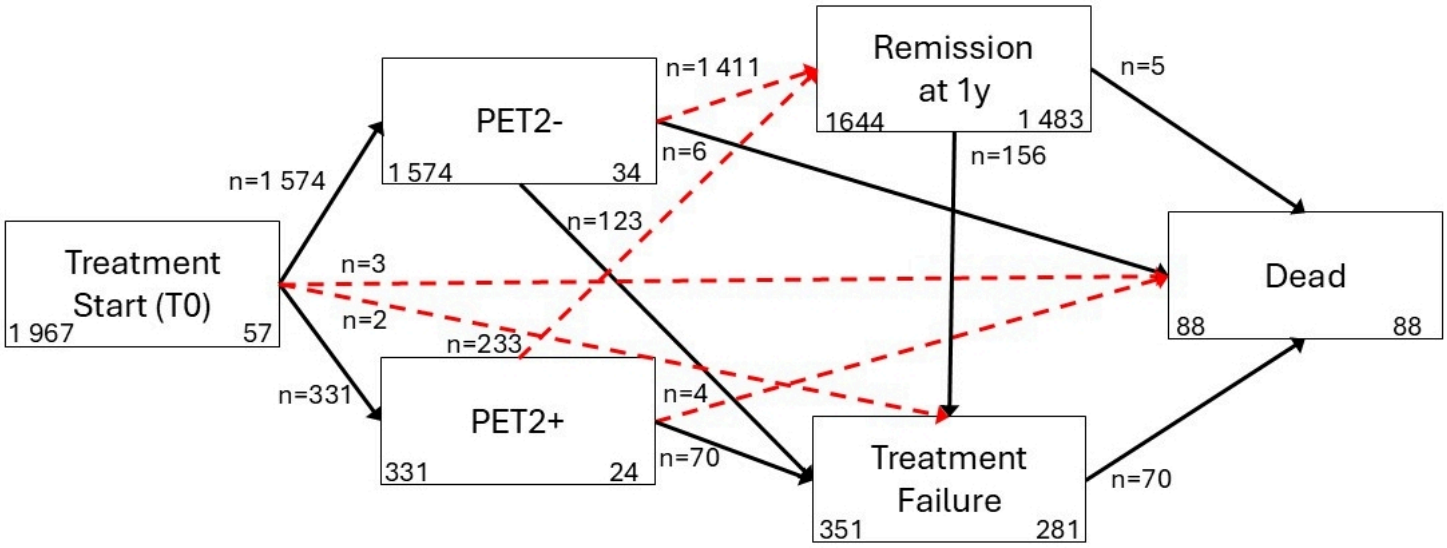

Figure 1

MSM illustrating disease states and transitions across the 5-year cHL post-acute disease trajectory

Number in lower left indicates number entering that state; number in lower right indicates number remaining in state (typically due to censoring; see Table S3); number on pathway indicates number transition between states. Red dashed lines indicate transitions not modeled in the analysis describing their associations with covariates due to small N or artificial entry into the state at 1 year (remission at 1y).

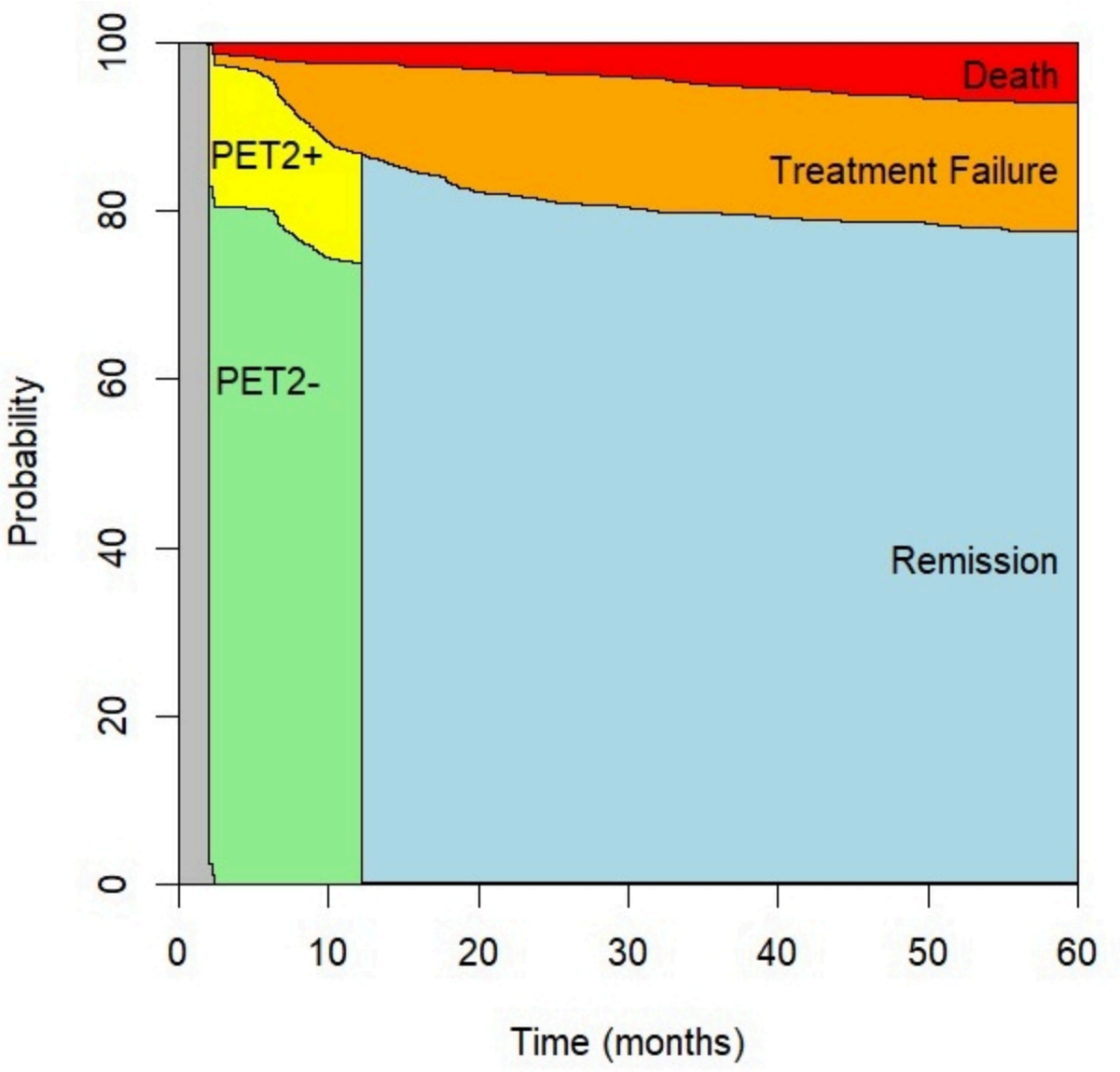

Figure 2

MSM disease state probabilities over time

This state occupancy plot indicates the probability (y-axis) of being in a given MSM disease state (represented by different colors) over time (x-axis). All patients start in the grey “Treatment Start (T0)” state until PET2 at 60 day or an early event (whichever occurs first). At 60 days, most patients enter the PET2+ (yellow) or PET2- (green) state. Patients remaining alive and event-free at 1 year enter the remission state (blue). Over the 5-year time period, patients may experience treatment failure (orange) or death (red).

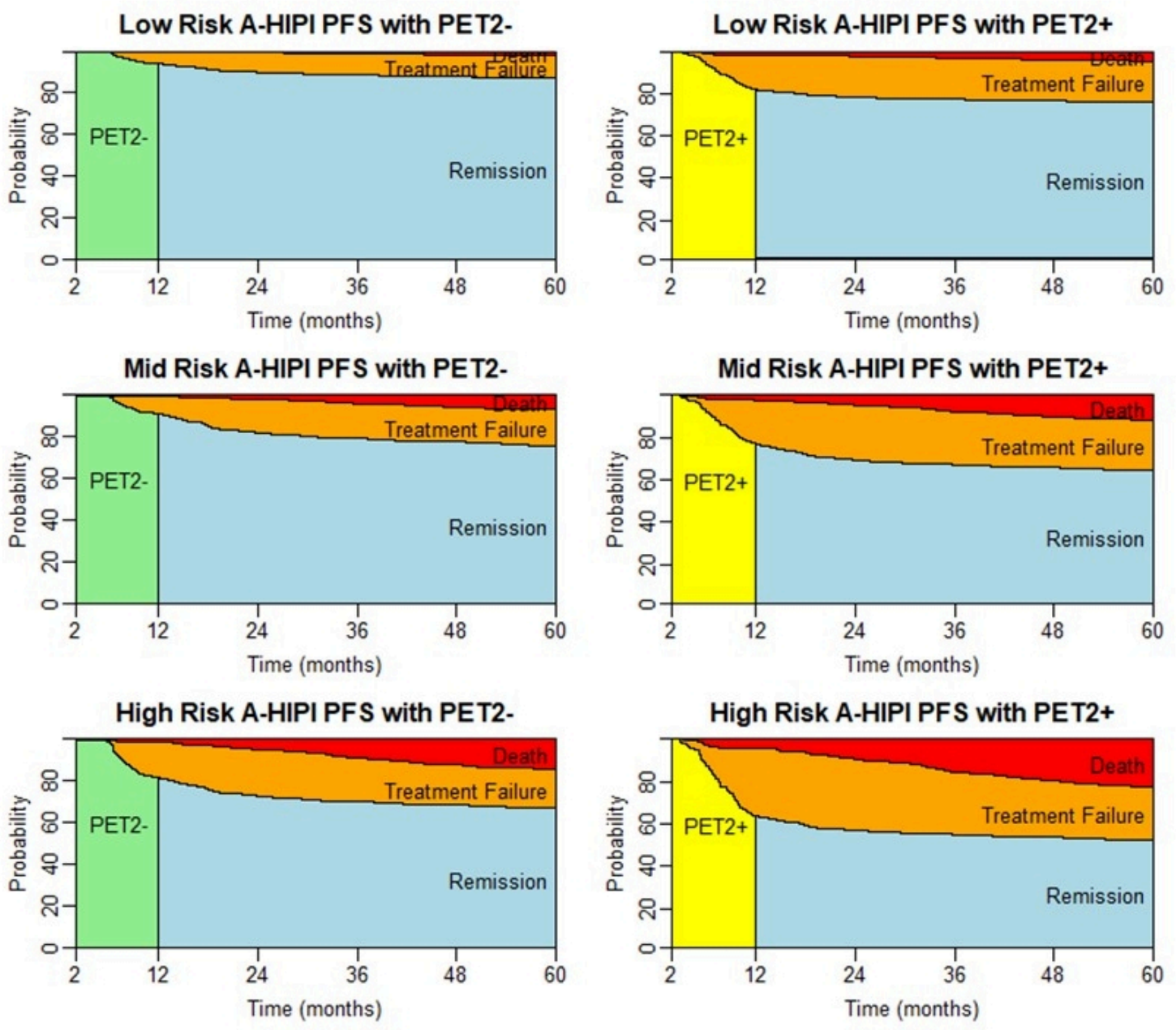

Figure 3

MSM disease state probabilities over time by tertiles of the A-HIPI PFS scores and PET2 result

These state occupancy plots indicate the probability (y-axis) of being in a given MSM disease state (represented by different colors) over time (x-axis) by A-HIPI tertile (low risk, mid risk, high risk) and PET2 result (negative, positive). All patients start in their respective PET2 state at 60 days (negative=green, positive=yellow). Patients remaining alive and event-free at 1 year enter the remission state (blue). Over the 5-year time period, patients may experience treatment failure (orange) or death (red).

Supplementary Files

This is a list of supplementary files associated with this preprint. Click to download.

- SupplementaryInformation.pdf